4. The Mulliken charges of copper ions and lattice ion distortions are strongly coupled. Disproportionation of copper ions is not favored energetically, but an internal complex involving ions representing Cu^+ at site 1 and Cu^{3+} at site 4 is nearly stable.

Appendix

The parameters we have employed are noted in Table VI. Note that the Cu and O ions are treated as suspended in an almost ionic lattice due to the appropriate combinations of Y^{3+}, La^{3+}, or Ba^{2+} ions. Then the additional classical terms due to the charges of ions not present in the cluster are added as Madelung-like terms in eq 2. This classical term does not fully account for termination of the cluster within a periodic field. Earlier work[13] has shown that a significantly reduced value must be chosen to determine effective charges of ions in the external field. A value of 0.23 was employed for LiF. In the case of these copper ion clusters we found that 0.18 was the largest value that would consistently give a converged SCF calculation and we employ this value in all calculations.

We may test whether the charge distribution in the external field is responsible for the effects on cluster charges and oxygen ion vacancy formation energy that we observe. We have thus performed calculations using the Madelung constants for the different external fields from Table II and in the absence of an external field. The results for oxygen vacancy formation and populations are shown in Table VII. In the case of oxygen vacancies the most favorable site for formation is in the chain (O_1). The site in the plane (O_3) is generally least favorable. The Mulliken charges are rather insensitive to the external field. Thus, the intrinsic cluster rather than the external field is dominant in determining these properties. Further calculations of the oxygen vacancy formation energy by the atomistic approach[11] are consistent with O_1 vacancy formation most easily for each of these potential models.

Contribution from the Department of Chemistry and Biochemistry, University of Colorado, Boulder, Colorado 80309

Divalent Rhenium Coordination to Two Radical Schiff-Base Quinone Ligands

Lynn A. deLearie, R. Curtis Haltiwanger, and Cortlandt G. Pierpont*

Received April 12, 1988

Reactions of $Re(CO)_5Br$ and $Re_2(CO)_{10}$ with 3,5-di-*tert*-butylcatechol and ammonia have been investigated. Related reactions carried out with divalent first-row transition-metal ions gave $M^{II}(Cat\text{-}N\text{-}BQ)_2$ compounds, where Cat-N-BQ is a biquinone ligand formed from Schiff-base condensation reactions of 3,5-di-*tert*-butylcatechol and ammonia. In contrast, these reactions produced $Re(CO)_3(C_{28}H_{39}NO_2)(C_{14}H_{21}NO)$, a complex of divalent rhenium with three carbonyl ligands, one anionic monodentate 3,5-di-*tert*-butyl-2-iminophenolate ligand, and one anionic chelating 1-hydroxy-2,4,6,8-tetra-*tert*-butylphenoxazinyl ligand. The complex crystallizes in the triclinic space group $P\bar{1}$ with two complex molecules of slightly different structures per asymmetric unit and unit cell dimensions of a = 12.153 (6) Å, b = 16.376 (14) Å, c = 24.428 (14) Å, α = 107.13 (6)°, β = 102.08 (4)°, γ = 88.85 (6)°, and V = 4539 (5) Å^3. The paramagnetic Re(II) complex exhibits a unique charge distribution, with radical localization on the phenoxazinyl ligand and strong antiferromagnetic coupling between the metal and the radical iminophenolate ligand. The solid-state magnetic moment of 1.31 (2) μ_B is consistent with a spin-orbit-coupled radical, and the isotropic EPR spectrum confirms radical localization on the phenoxazinyl ligand. Mechanistic implications for formation of both radical ligands as well as previously characterized Cat-N-BQ ligands are discussed.

Introduction

Rhenium forms few compounds in the divalent oxidation state, and this is the most poorly characterized of its eight oxidation levels.[1] As with the other lower oxidation states, divalent rhenium shows a tendency to form metal-metal bonds, and much of its chemistry has been focused on the characterization of diamagnetic binuclear phosphine complexes.[2] Mononuclear coordination compounds of rhenium(II) are much less common, again with most containing mono- or bidentate phosphine and arsine ligands.[1b,3] These compounds are paramagnetic with low-spin d^5 configurations, and some, such as *trans*-$ReCl_2(CO)_2(P(n\text{-}Pr)_3)_2$, exhibit EPR spectra characteristic of metal-localized radicals.[3a] In this report we discuss reactions of $Re(CO)_5Br$ with 3,5-di-*tert*-butylcatechol and aqueous ammonia in air, which resulted in formation of a divalent rhenium tricarbonyl complex containing 3,5-di-*tert*-butyl-2-iminophenolate and 1-hydroxy-2,4,6,8-tetra-*tert*-butylphenoxazinylate ligands. Coordination of divalent rhenium to paramagnetic ligands has not been demonstrated previously, and complexation of the iminophenolate and phenoxazinyl radical ligands in the title compound is the first well-characterized example of this coordination.

Scheme I

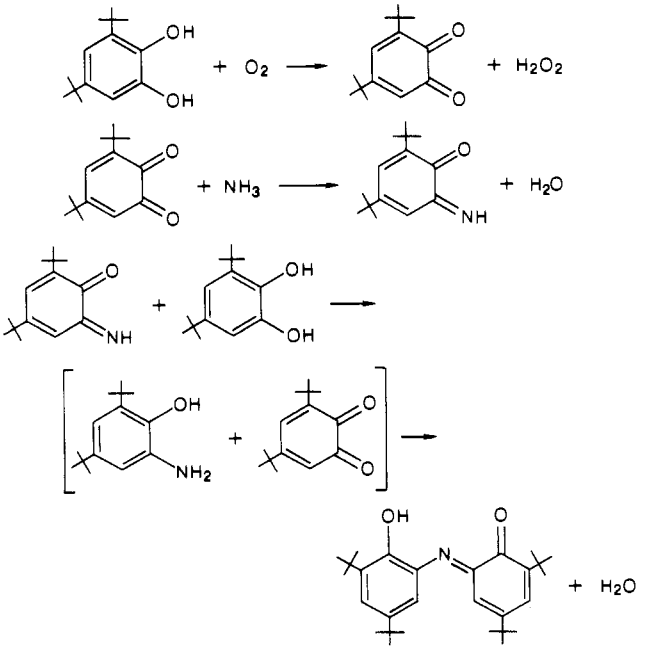

(1) (a) Turp, J. E. *Coord. Chem. Rev.* **1983**, *53*, 249. (b) Fergusson, J. E. *Coord. Chem. Rev.* **1966**, *1*, 459.
(2) (a) Cotton, F. A.; Wilkinson, G. *Advanced Inorganic Chemistry*, 4th ed.; John Wiley and Sons, Inc.: New York, 1980. (b) Heveldt, P. F.; Watson, D. J. *Inorg. Chem. Transition Elem.* **1978**, *6*, 85. (c) Ebner, J. R.; Walton, R. A. *Inorg. Chem.* **1975**, *14*, 1987. (d) Chatt, J.; Rowe, G. A. *J. Inorg. Nucl. Chem.* **1962**, 4019.
(3) (a) Hertzer, C. A.; Myers, R. E.; Brant, P.; Walton, R. A. *Inorg. Chem.* **1978**, *17*, 2383. (b) Chatt, J.; Dilworth, J. R.; Gunz, H. P.; Leigh, G. J. *J. Organomet. Chem.* **1974**, *64*, 245. (c) Chatt, J.; Rowe, G. A. *Chem. Ind.* **1962**, 92. (d) Curtis, N. F.; Fergusson, J. E.; Nyholm, R. S. *Chem. Ind.* **1958**, 625.

0020-1669/89/1328-0644$01.50/0 © 1989 American Chemical Society

Recent investigations of reactions between 3,5-di-*tert*-butylcatechol, divalent metal ions, and aqueous ammonia in air have shown that bis complexes of the 3,5-di-*tert*-butyl-1,2-quinone 1-(2-hydroxy-3,5-di-*tert*-butylphenyl)imine (Cat-N-BQ) ligand are formed.[4] Girgis proposed that formation of this ligand proceeded through reactions outlined in Scheme I, involving initial generation of a quinone imine followed by further Schiff-base condensation to form the tridentate biquinone.[4b]

It was also suggested that only the 2,4-di-*tert*-butyliminoquinone isomer was formed due to steric constraints of 3,5-di-*tert*-butylcatechol. In the present study we have found that both the 3,5-di-*tert*-butyl-2-iminophenolate and 1-hydroxy-2,4,6,8-tetra-*tert*-butylphenoxazinyl ligands in $Re(CO)_3(C_{14}H_{21}NO)(C_{28}H_{39}NO_2)$ are also formed from Schiff-base condensation reactions of 3,5-di-*tert*-butylcatechol and ammonia. Investigation of the chemistry leading to this compound is important in elucidation of the reaction mechanism involved in formation, as well as further rearrangements, of the Cat-N-BQ ligands.

Experimental Section

$Re_2(CO)_{10}$ was obtained from Strem Chemical Co. and was used as received. $Re(CO)_5Br$ was synthesized from $Re_2(CO)_{10}$ and Br_2 according to a previously published procedure[5] and was sublimed before use. 3,5-Di-*tert*-butylcatechol and 3,5-di-*tert*-butyl-1,2-benzoquinone was obtained from Aldrich Chemical Co., NH_4OH was obtained from Mallinckrodt Chemical Co., and all were used as received. $(CH_3)_3NO{\cdot}2H_2O$ was obtained from Eastman Organic Chemicals and was sublimed before use. Reactions requiring photolysis were carried out under an atmosphere of N_2, reaction with $(CH_3)_3NO$ was carried out under Ar, and all other reactions were performed in air at room temperature.

Synthesis of $Re(CO)_3(C_{14}H_{21}NO)(C_{28}H_{39}NO_2)$. $Re(CO)_5Br$ (0.55 g, 1.35 mmol) was dissolved in a mixture of 80 mL of CH_2Cl_2 and 40 mL of 95% ethanol. 3,5-Di-*tert*-butylcatechol (0.66 g, 2.97 mmol) was dissolved in 40 mL of CH_2Cl_2 and added to the solution. Concentrated NH_4OH (20 mL) in 50 mL of 95% ethanol was added to the mixture, and the resulting solution was stirred in air at room temperature for 24 h. The maroon product was extracted into pentane after complete evaporation of the reaction solution and was isolated in nearly quantitative yield after recrystallization from CH_2Cl_2/ethanol. A similar procedure using $Re_2(CO)_{10}$ (0.52 g, 0.80 mmol), 3,5-di-*tert*-butylcatechol (0.80 g, 3.60 mmol), and ammonia also gave quantitative yields of product.

Anal. Calcd for $ReC_{45}H_{60}N_2O_6$: C, 59.32; H, 6.64; N, 3.07. Found: C, 59.42; H, 6.68; N, 3.07.

Reaction of $Re(CO)_3(C_{14}H_{21}NO)(C_{28}H_{39}NO_2)$ with $(CH_3)_3NO$. $Re(CO)_3(C_{14}H_{21}NO)(C_{28}H_{39}NO_2)$ (0.22 g, 0.25 mmol) and $(CH_3)_3NO$ (0.018 g, 0.25 mmol) were dissolved in 50 mL of freshly distilled CH_2Cl_2 and freeze–thaw–degassed for two cycles under Ar. The resulting solution was stirred for 24 h at room temperature. Another equivalent of $(CH_3)_3NO$ (0.020 g) was added under Ar, and the resulting solution was refluxed for 48 h. No reaction was observed.

Photolytic Reaction of $Re(CO)_5Br$, 3,5-DBCat, 3,5-DBBQ, and Ammonia. $Re(CO)_5Br$ (0.66 g; 1.63 mmol) was dissolved in a mixture of 80 mL of CH_2Cl_2 and 40 mL of 95% ethanol. 3,5-Di-*tert*-butylcatechol (0.40 g; 1.79 mmol) and 3,5-di-*tert*-butyl-1,2-benzoquinone (0.39 g; 1.79 mmol) were dissolved in 40 mL of CH_2Cl_2 and added to the above solution. Concentrated NH_4OH (20 mL) in 50 mL of 95% ethanol was added to the above, and the resulting solution was photolyzed under N_2 at 0 °C for 6 h with an Ace Glass Inc. 700-W mercury vapor lamp. The product was detected in minimal yields through spectroscopic techniques. A similar procedure using $Re_2(CO)_{10}$ also resulted in product formation.

Physical Measurements. Infrared spectra were recorded on an IBM IR/30 Series FTIR spectrometer with samples prepared as KBr pellets. UV/vis spectra were recorded on a Hewlett Packard 8451A diode-array spectrophotometer. Magnetic susceptibility measurements were made by the Faraday technique on a Sartorius 4433 microbalance, and electron paramagnetic resonance spectra were obtained on a Varian E-109 spectrometer with DPPH used as the g value standard. Mass spectra were recorded on a VG Analytical 7070 EQ mass spectrometer. Cyclic voltammograms were obtained with a BAS-100 electrochemical analyzer in CH_2Cl_2 solutions. A platinum disk working electrode and a platinum wire counter electrode were used. The reference electrode was based on the Ag/Ag^+ couple and consisted of a CH_2Cl_2 solution of silver hexafluorophosphate in contact with a silver wire placed in glass tubing with a Vycor frit at one end to allow ion transport. Tetrabutylammonium hexafluorophosphate was used as the supporting electrolyte, and the ferrocene/ferrocenium couple was used as the internal standard. Controlled-potential electrolysis was performed in CH_2Cl_2 solutions by using a PAR Model 173 potentiostat with a PAR Model 175 Universal programmer. A platinum-gauze working electrode and a platinum-wire counter electrode were used. The counter electrode was separated from the bulk solution with a Vycor frit. The reference electrode was identical with that used for cyclic voltammetry, and tetrabutylammonium hexafluorophosphate was used as the supporting electrolyte.

Crystallographic Structure Determination. All crystals isolated were soft and deteriorated when removed from the CH_2Cl_2/ethanol solutions. A crystal was mounted on a glass fiber, coated with an amorphous resin to prevent crystal deterioration, and aligned on a Nicolet P3F automated diffractometer. Axial and rotational photographs indicated triclinic symmetry for the crystal. Unit cell dimensions given in Table I were calculated from the centered positions of 15 intense reflections with $20.0° \leq 2\theta \leq 25.0°$. Details of procedures used for data collection and structure determination are given in Table I.

Positions of the two independent Re atoms were determined from a three-dimensional Patterson map. Phases derived from the Re positions were used to locate all other non-hydrogen atoms of the structure. The final cycles of least-squares refinement were refined in blocks of 403–409 parameters per cycle. Both Re atoms and all carbonyl ligands were refined in all cycles; refinement of the two different phenoxazinyl radical ligands and both *o*-iminophenolate ligands alternated in different cycles. The final cycles of refinement converged with discrepency indices of $R = 0.064$ and $R_w = 0.078$. Maximum residual electron density of 2.90 e/Å^3 was observed 1.18 Å from Re. Final positional and isotropic thermal parameters for all non-hydrogen atoms are listed in Table II. Tables containing anisotropic thermal parameters and structure factors are available as supplementary material.

Table I. Crystal Data and Details of the Structure Determination and Refinement for $Re(CO)_3(C_{28}H_{39}NO_2)(C_{14}H_{21}NO)$

chem formula	$ReC_{45}H_{60}N_2O_6$
fw	911.2
space group	$P\bar{1}$
a, Å	12.153 (6)
b, Å	16.376 (14)
c, Å	24.428 (14)
α, deg	107.13 (6)
β, deg	102.08 (4)
γ, deg	88.85 (6)
V, Å^3	4539 (5)
Z	4
Temp, K	294–297
γ, Å	Mo Kα (0.71069)
ρ_{meas}, g/cm^3	1.32 (2)
ρ_{calc}, g/cm^3	1.33
μ, cm^{-1}	27.29
transmissn coeff	0.872–0.469
R	0.0643
R_w	0.0783

Experimental Results

The $Re(CO)_3(C_{14}H_{21}NO)(C_{28}H_{39}NO_2)$ complex has been prepared by room-temperature reactions of both $Re(CO)_5Br$ and $Re_2(CO)_{10}$ with 3,5-di-*tert*-butylcatechol and ammonium hydroxide. Dark maroon crystals suitable for X-ray crystallographic analysis were obtained by recrystallization of the crude product from a methylene chloride/ethanol solution.

Reaction with trimethylamine *N*-oxide was followed with solution EPR spectroscopy, and the final crude products were analyzed by FTIR spectroscopy. No reaction was observed after 24 h at room temperature, and only minimal dissociation of phenoxazinyl radical ligands was observed after refluxing in methylene chloride. No reduction in carbonyl stretching frequencies in the crude product was observed, indicating that carbonyl ligand oxidation did not occur under these conditions.

Photolytic reactions of both $Re(CO)_5Br$ and $Re_2(CO)_{10}$ in the presence of equimolar quantities of 3,5-di-*tert*-butylcatechol and 3,5-di-*tert*-butyl-1,2-benzoquinone, and ammonium hydroxide were also studied. Presence of the $Re(CO)_3(C_{14}H_{21}NO)(C_{28}H_{39}NO_2)$ complex was established from EPR and UV/vis spectra recorded on the reaction solutions. No evidence was found to indicate that

(4) (a) Larsen, S. K.; Pierpont, C. G. *J. Am. Chem. Soc.* **1988**, *110*, 1827. (b) Girgis, A. Y.; Balch, A. L. *Inorg. Chem.* **1975**, *14*, 2724.
(5) Michels, G. D; Svec, H. J. *Inorg. Chem.* **1981**, *20*, 3445.

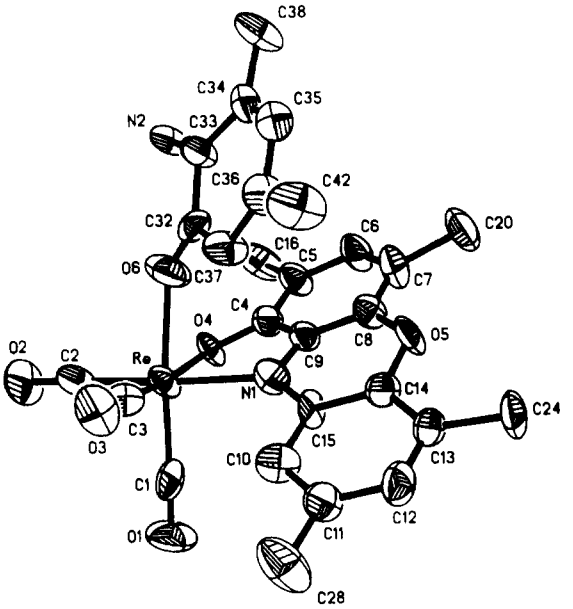

Figure 1. Plot showing the structure of one of the molecules in the asymmetric unit of $Re(CO)_3(C_{14}H_{21}NO)(C_{28}H_{39}NO_2)$. The methyl carbon atoms have been omitted for clarity.

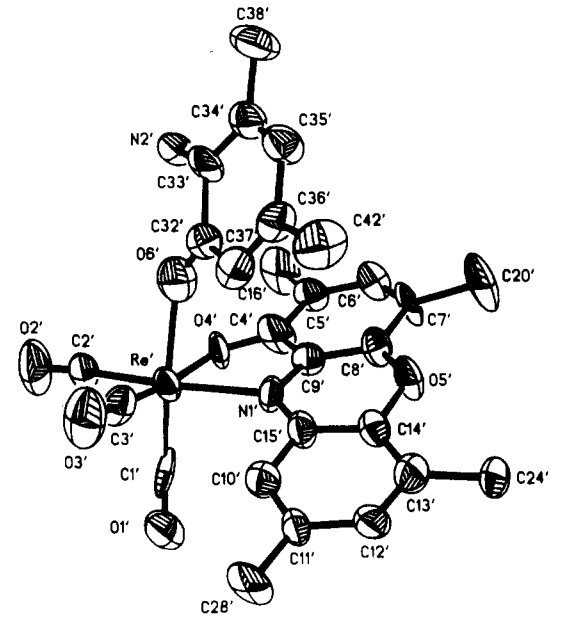

Figure 2. Plot showing the second molecule in the asymmetric unit of $Re(CO)_3(C_{14}H_{21}NO)(C_{28}H_{39}NO_2)$.

further carbonyl ligand cleavage occurred under these reaction conditions.

Crystallographic Characterization of $Re(CO)_3(C_{14}H_{21}NO)(C_{28}H_{39}NO_2)$. The complex was found to crystallize in the triclinic space group $P\bar{1}$, with two independent molecules per asymmetric unit. Figures 1 and 2 contain views of the independent molecules, and selected bond lengths and angles of the structure are listed in Table III. The coordination geometry about both rhenium atoms is octahedral, showing only slight distortions arising from chelation constraints of the phenoxazinyl radical ligands. Bond angles of 75.4 (5) and 75.6 (5)° for O4–Re–N1 and O4′–Re′–N1′ angles, respectively, show the greatest distortions from a regular octahedron.

The two independent molecules differ structurally in the projection of the iminophenolate ligand plane on the tetragonal plane of the complex containing the phenoxazinyl ligand. The angle θ shown below between the plane of the iminophenolate ligand and the Re–C3 bond is 44.2° and the same angle in the other independent molecule is 34.3°.

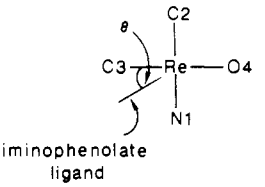

Carbonyl bonding is linear with average Re–C–O bond angles of 176.7 (16)°, average Re–C bond lengths of 1.893 (19) Å, and average C–O bond lengths of 1.170 (25) Å. This Re–C length is nearly 0.1 Å shorter than the only other rhenium(II) carbonyl length of 1.980 (17) Å reported for $Re(CO)_2(PEt_3)_2Cl_2$.[6]

Bond lengths of the *o*-iminophenolate ligand are consistent with charge localization within the ring (I). The C34–C35 and

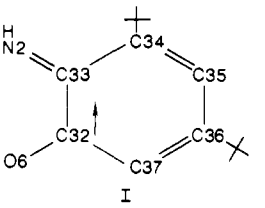

I

C36–C37 bond lengths and their primed equivalents in the second molecule are short, averaging to 1.348 (29) and 1.369 (27) Å, respectively, for the two independent molecules, suggesting localized double bonds. The C32–C33 bond lengths in both molecules are long, averaging to 1.572 (28) Å, and are consistent with a single bond between these atoms and localization of a radical on C32. Carbon–oxygen bond lengths of 1.329 (25) Å and 1.304 (20) Å for C32–O6 and C32′–O6′, respectively, are slightly shorter than single C–O lengths usually found for coordinated catecholate ligands, and suggest some delocalization of the radical into this bond.[7] Rhenium–oxygen bond lengths of 2.168 (11) and 2.157 (16) Å for Re–O and Re′–O′ are significantly longer than Re(VI)–O bond lengths to catecholate ligands in either $Re^{VI}(3,5\text{-DBCat})_3$ or $Re^{VI}(Cl_4Cat)_3$,[8] and are consistent with bonding to a lower valent metal ion. Carbon–nitrogen bond lengths of 1.159 (27) and 1.178 (28) Å for C33–N2 and C33′–N2′, respectively, are extremely short. Refinement of these atoms as nitrogens was questionable because neither hydrogen positions nor slight differences between the thermal parameters of nitrogen and oxygen atoms could be determined due to insufficient structural resolution. However, analytical data confirmed the presence of two nitrogen atoms per molecule, and infrared N–H stretching vibrations showed that the nitrogen was not coordinated to the metal; structure refinement was completed with nitrogen atoms in these positions.

Bonding of the iminophenolate ligand is also unique due to the monodentate coordination. Such coordination of a potentially chelating ligand is rare, and similar behavior has previously been observed in [*N*,*N*′-(1,2-phenylene)bis(salicylideneaminato)](catecholato-*O*)iron(III).[9] In the Fe(saloph)CatH complex, the quinone is in the fully reduced catecholate state, and bond lengths within this ligand are consistent with such a charge formulation; carbon–oxygen bond lengths to the coordinating and unbound oxygen atoms are 1.352 and 1.360 Å, respectively. Bonding of the iminophenolate ligand in the rhenium complex differs slightly because the ligand in a partially reduced radical form that would be equivalent to the semiquinone form of *o*-benzoquinones.

Coordination of the radical, 1-hydroxy-2,4,6,8-tetra-*tert*-butylphenoxazinyl, to a variety of organometallic compounds has previously been studied by EPR spectroscopy, and it was proposed

(6) Bucknor, S.; Cotton, F. A.; Falvello, L. R.; Reid, A. H., Jr.; Schmulbach, C. D. *Inorg. Chem.* **1986**, *25*, 1021.
(7) Pierpont, C. G.; Buchanan, R. M. *Coord. Chem. Rev.* **1981**, *38*, 45.
(8) (a) deLearie, L. A.; Pierpont, C. G. *J. Am. Chem. Soc.* **1986**, *108*, 6393. (b) deLearie, L. A.; Haltiwanger, R. C.; Pierpont, C. G. *Inorg. Chem.* **1987**, *26*, 817.
(9) (a) Que, L., Jr. *Coord. Chem. Rev.* **1983**, *50*, 73. (b) Heistand, R. H., II; Lauffer, R. B.; Fikrig, E.; Que, L., Jr. *J. Am. Chem. Soc.* **1982**, *104*, 2789. (c) Heistand, R. H., II; Roe, A. L.; Que, L., Jr. *Inorg. Chem.* **1982**, *21*, 676.

Table II. Atomic Coordinates ($\times 10^4$) and Equivalent Isotropic Displacement Parameters ($A^2 \times 10^3$) for $Re(CO)_3(C_{28}H_{39}NO_2)(C_{14}H_{21}NO)$

	x/a	y/b	z/c	U(eq)[a]		x/a	y/b	z/c	U(eq)[a]
Re	292 (1)	2379 (1)	2789 (1)	43 (1)	C37	−1758 (14)	1280 (13)	3222 (7)	59 (9)
Re′	4157 (1)	2175 (1)	7820 (1)	45 (1)	C38	−5421 (14)	1171 (14)	2343 (9)	70 (10)
O1	2607 (11)	3302 (10)	3316 (6)	85 (7)	C39	−6174 (16)	986 (18)	2766 (10)	103 (14)
O2	1005 (11)	1670 (10)	1603 (5)	83 (7)	C40	−5650 (16)	426 (14)	1743 (9)	81 (10)
O3	1259 (11)	803 (9)	3100 (6)	79 (7)	C41	−5698 (17)	2064 (13)	2254 (10)	82 (11)
O4	−647 (8)	3387 (7)	2579 (4)	45 (5)	C42	−2361 (17)	700 (16)	3981 (9)	82 (11)
O5	−1628 (9)	3687 (8)	4410 (5)	54 (5)	C43	−2689 (21)	−262 (15)	3776 (10)	106 (13)
O6	−1410 (9)	1824 (8)	2451 (6)	73 (6)	C44	−3075 (24)	1239 (21)	4428 (10)	137 (17)
O1′	7070 (11)	9433 (10)	2163 (7)	80 (7)	C45	−1063 (20)	806 (18)	4266 (11)	120 (15)
O2′	2140 (12)	2486 (12)	6928 (7)	105 (9)	C1′	6598 (16)	8820 (12)	2198 (7)	54 (8)
O3′	2932 (13)	3256 (10)	8732 (7)	96 (8)	C2′	2911 (15)	2376 (13)	7238 (8)	61 (9)
O4′	5146 (8)	1593 (7)	7209 (5)	52 (5)	C3′	3405 (15)	2822 (12)	8381 (8)	54 (8)
O5′	7856 (8)	1593 (8)	8901 (5)	57 (5)	C4′	6200 (15)	1557 (15)	7422 (8)	73 (10)
O6′	5139 (11)	3256 (9)	7814 (7)	82 (7)	C5′	7065 (14)	1460 (12)	7121 (7)	54 (8)
N1	−331 (11)	3012 (9)	3566 (6)	47 (6)	C6′	8187 (15)	1428 (13)	7414 (9)	66 (9)
N2	−3530 (10)	1464 (9)	1841 (6)	45 (6)	C7′	8506 (13)	1485 (14)	8004 (9)	68 (10)
N1′	5680 (10)	1841 (9)	8346 (6)	48 (6)	C8′	7644 (13)	1563 (11)	8320 (7)	50 (8)
N2′	6123 (11)	4365 (10)	7440 (6)	52 (7)	C9′	6501 (14)	1653 (12)	8045 (7)	51 (8)
C1	1750 (17)	2980 (11)	3127 (7)	50 (8)	C10′	4995 (14)	1858 (12)	9188 (8)	53 (8)
C2	709 (13)	1937 (12)	2048 (8)	52 (8)	C11′	5165 (12)	1758 (11)	9760 (7)	48 (8)
C3	895 (15)	1440 (14)	2973 (9)	66 (8)	C12′	6262 (14)	1583 (12)	10021 (8)	57 (8)
C4	−1406 (13)	3649 (11)	2898 (7)	47 (7)	C13′	7154 (15)	1487 (12)	9744 (8)	60 (9)
C5	−2369 (13)	4097 (12)	2740 (7)	53 (8)	C14′	6960 (13)	1618 (10)	9194 (7)	46 (7)
C6	−3101 (14)	4311 (12)	3146 (8)	58 (9)	C15′	5896 (13)	1810 (11)	8904 (7)	50 (8)
C7	−2896 (15)	4170 (12)	3687 (8)	58 (9)	C16′	6768 (18)	1337 (19)	6437 (10)	96 (13)
C8	−1934 (13)	3793 (11)	3843 (7)	45 (7)	C17′	7952 (19)	1214 (18)	6218 (10)	114 (14)
C9	−1222 (13)	3476 (11)	3460 (7)	43 (7)	C18′	5938 (21)	585 (17)	6097 (11)	111 (13)
C10	1067 (15)	2577 (11)	4284 (8)	54 (8)	C19′	6311 (19)	2222 (18)	6379 (11)	102 (14)
C11	1451 (14)	2604 (12)	4873 (7)	54 (8)	C20′	9791 (15)	1513 (19)	8324 (11)	101 (14)
C12	835 (15)	2996 (12)	5298 (7)	58 (8)	C21′	10027 (18)	722 (18)	8543 (12)	113 (15)
C13	−174 (14)	3368 (11)	5164 (7)	47 (7)	C22′	10074 (16)	2409 (18)	8826 (11)	99 (13)
C14	−585 (14)	3337 (12)	4573 (7)	50 (8)	C23′	10527 (16)	1533 (24)	7832 (12)	151 (20)
C15	48 (14)	2986 (11)	4143 (7)	43 (7)	C24′	8303 (15)	1154 (16)	10010 (9)	78 (11)
C16	−2639 (14)	4263 (15)	2148 (10)	75 (11)	C25′	8477 (19)	251 (16)	9601 (12)	105 (13)
C17	−3825 (17)	4654 (17)	2028 (10)	97 (13)	C26′	9258 (17)	1830 (16)	10123 (11)	105 (13)
C18	−1751 (17)	4981 (16)	2153 (10)	94 (12)	C27′	8263 (16)	1074 (17)	10644 (9)	94 (12)
C19	−2638 (19)	3412 (15)	1631 (8)	86 (11)	C28′	4198 (15)	1882 (17)	10097 (9)	79 (11)
C20	−3820 (16)	4411 (16)	4065 (9)	80 (11)	C29′	4341 (21)	1282 (26)	10483 (15)	184 (26)
C21	−4873 (16)	4820 (16)	3758 (10)	96 (13)	C30′	4318 (27)	2787 (25)	10532 (16)	194 (24)
C22	−3322 (18)	5103 (16)	4663 (10)	96 (12)	C31′	3067 (19)	1729 (26)	9687 (11)	167 (21)
C23	−4294 (17)	3534 (16)	4129 (12)	102 (14)	C32′	5866 (15)	3822 (11)	8201 (8)	48 (8)
C24	−768 (16)	3875 (13)	5660 (8)	65 (9)	C33′	6474 (15)	4404 (13)	7934 (10)	64 (10)
C25	−2037 (17)	3484 (14)	5547 (9)	78 (10)	C34′	7404 (15)	4934 (12)	8357 (9)	59 (9)
C26	−697 (19)	4825 (15)	5701 (10)	95 (12)	C35′	7707 (15)	4928 (13)	8921 (8)	64 (9)
C27	−87 (19)	3763 (19)	6261 (8)	111 (13)	C36′	7047 (16)	4402 (12)	9156 (7)	53 (8)
C28	2537 (17)	2123 (17)	5021 (10)	87 (12)	C37′	6140 (16)	3886 (12)	8815 (8)	60 (9)
C29	3401 (16)	2259 (18)	4684 (11)	108 (15)	C38′	8088 (19)	5487 (16)	8107 (11)	91 (12)
C30	3081 (25)	2455 (22)	5670 (11)	152 (18)	C39′	7241 (21)	6203 (16)	7980 (12)	104 (14)
C31	2194 (21)	1157 (17)	4845 (14)	121 (17)	C40′	1485 (19)	5050 (16)	2448 (11)	97 (13)
C32	−2103 (14)	1453 (10)	2672 (7)	44 (8)	C41′	9163 (20)	5928 (17)	8587 (10)	108 (13)
C33	−3341 (13)	1380 (12)	2305 (9)	54 (9)	C42′	7463 (20)	4503 (15)	9819 (9)	81 (11)
C34	−4149 (14)	1182 (12)	2639 (8)	53 (8)	C43′	7693 (33)	5422 (18)	10173 (11)	162 (20)
C35	−3798 (14)	1002 (11)	3145 (8)	51 (8)	C44′	8528 (22)	4026 (17)	9888 (10)	121 (14)
C36	−2604 (15)	1026 (12)	3439 (7)	54 (8)	C45′	6537 (20)	4089 (21)	10047 (10)	126 (16)

[a] Equivalent isotropic U defined as one-third of the trace of the orthogonalized U_{ij} tensor.

that chelation through the deprotonated hydroxy oxygen atom and the nitrogen atom occurred.[10] This report includes the first structural characterization of such a complex, and chelation to the rhenium atom is confirmed. Rhenium–oxygen bond lengths of 2.115 (11) and 2.106 (11) Å for Re–O4 and Re′–O4′, respectively, are shorter than the Re–O bond lengths of the *o*-iminophenolate ligands. Carbon–oxygen bond lengths of 1.313 (20) and 1.286 (20) Å for C4–O4 and C4′–O4′, respectively, are shorter than single C–O lengths usually found for coordinated catecholate ligands. Carbon–nitrogen bond lengths within the chelate ring of 1.336 (21) and 1.337 (23) Å for N1–C9 and N1′–C9′, respectively, are shorter than carbon–nitrogen lengths outside the chelate of 1.405 (22) and 1.353 (24) Å for N1–C15 and N1′–C15′, respectively. Both features can be explained by delocalization of the oxygen anion and the phenoxazinyl radical throughout the chelate ring (II).

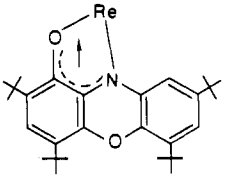

II

Spectroscopic Properties of $Re(CO)_3(C_{14}H_{21}NO)(C_{28}H_{39}NO_2)$. The infrared spectrum of this complex shows many similarities to the spectra of several $M^{II}(Cat\text{-}N\text{-}BQ)_2$ complexes as well as to the spectrum of phenoxazine.[4,11] Major spectral features above 1200 cm^{-1} include an imine N–H stretching frequency at 3204

(10) Karsanov, I. V.; Ivakhnenko, E. P.; Khandkarova, V. S.; Rubezhov, A. Z.; Okhlobystin, O. Yu.; Minkin, V. I.; Prokof'ev, A. I.; Kabachnik, M. I. *Izv. Akad. Nauk SSSR, Ser. Khim.* **1987**, 56.

(11) Pouchert, C. J. *The Aldrich Library of Infrared Spectra*, 3rd ed.; Aldrich Chemical Co.: Milwaukee, WI, 1981; p 794.

Table III. Selected Bond Lengths (Å) and Angles (deg) for $Re(CO)_3(C_{28}H_{39}NO_2)(C_{14}H_{21}NO)$

	Rhenium Coordination		
	Bond Lengths		
Re–O4	2.115 (11)	Re′–O4′	2.106 (11)
Re–O6	2.168 (11)	Re′–O6′	2.157 (16)
Re–N1	2.158 (14)	Re′–N1′	2.185 (13)
Re–C1	1.941 (18)	Re′–C1′	1.870 (18)
Re–C2	1.912 (19)	Re′–C2′	1.949 (18)
Re–C3	1.825 (23)	Re′–C3′	1.861 (19)
	Bond Angles		
O6–Re–O4	76.3 (5)	O6′–Re′–O4′	78.1 (5)
N1–Re–O4	75.4 (5)	N1′–Re′–O4′	75.6 (5)
N1–Re–O6	84.2 (5)	N1′–Re′–O6′	86.6 (6)
C1–Re–O4	99.2 (6)	C1′–Re′–O4′	97.4 (6)
C1–Re–O6	174.3 (6)	C1′–Re′–O6′	175.2 (6)
C1–Re–N1	91.4 (6)	C1′–Re′–N1′	90.5 (6)
C2–Re–O4	95.8 (7)	C2′–Re′–O4′	94.7 (6)
C2–Re–O6	93.1 (6)	C2′–Re′–O6′	92.1 (8)
C2–Re–N1	171.2 (7)	C2′–Re′–N1′	170.3 (7)
C2–Re–C1	90.7 (7)	nC2′–Re′–C1′	90.1 (7)
C3–Re–O4	171.2 (7)	C3′–Re′–O4′	172.3 (7)
C3–Re–O6	95.5 (7)	C3′–Re′–O6′	94.3 (7)
C3–Re–N1	100.9 (8)	C3′–Re′–N1′	103.1 (7)
C3–Re–C1	88.8 (8)	C3′–Re′–C1′	90.2 (7)
C3–Re–C2	87.7 (9)	C3′–Re′–C2′	86.6 (8)
	Carbonyl Ligands		
	Bond Lengths		
O1–C1	1.119 (22)	O1′–C1′	1.199 (27)
O2–C2	1.173 (23)	O2′–C2′	1.125 (23)
O3–C3	1.223 (28)	O3′–C3′	1.182 (24)
	Bond Angles		
O1–C1–Re	177.7 (16)	O1′–C1′–Re′	174.8 (20)
O2–C2–Re	177.6 (13)	O2′–C2′–Re′	174.9 (20)
O3–C3–Re	177.5 (17)	O3′–C3′–Re′	177.9 (20)
	Phenoxazinyl Ligands		
	Bond Lengths		
O4–C4	1.313 (20)	O4′–C4′	1.286 (20)
O5–C8	1.420 (22)	O5′–C8′	1.376 (22)
O5–C14	1.412 (20)	O5′–C14′	1.415 (22)
N1–C9	1.336 (21)	N1′–C9′	1.337 (23)
N1–C15	1.405 (22)	N1′–C15′	1.353 (24)
C4–C5	1.416 (24)	C4′–C5′	1.385 (28)
C5–C6	1.431 (27)	C5′–C6′	1.411 (24)
C6–C7	1.381 (30)	C6′–C7′	1.391 (31)
C7–C8	1.350 (25)	C7′–C8′	1.408 (27)
C8–C9	1.388 (24)	C8′–C9′	1.438 (22)
C4–C9	1.458 (26)	C4′–C9′	1.452 (26)
C10–C11	1.408 (26)	C10′–C11′	1.429 (28)
C11–C12	1.401 (26)	C11′–C12′	1.417 (22)
C12–C13	1.380 (25)	C12′–C13′	1.376 (28)
C13–C14	1.415 (23)	C13′–C14′	1.397 (28)
C14–C15	1.409 (24)	C14′–C15′	1.417 (22)
C10–C15	1.424 (24)	C10′–C15′	1.402 (27)
	Bond Angles		
C4–O4–Re	113.2 (11)	C4′–O4′–Re′	115.8 (11)
C9–N1–Re	112.9 (11)	C9′–N1′–Re′	111.2 (11)
C15–N1–Re	129.6 (11)	C15′–N1′–Re′	130.4 (11)
C15–N1–C9	117.5 (14)	C15′–N1′–C9′	118.4 (14)
C14–O5–C8	119.1 (13)	C14′–O5′–C8′	120.6 (12)
	o-Iminophenolate Ligands		
	Bond Lengths		
O6–C32	1.329 (25)	O6′–C32′	1.304 (20)
N2–C33	1.159 (27)	N2′–C33′	1.178 (28)
C32–C33	1.570 (22)	C32′–C33′	1.573 (33)
C33–C34	1.494 (30)	C33′–C34′	1.458 (23)
C34–C35	1.341 (28)	C34′–C35′	1.354 (30)
C35–C36	1.476 (23)	C35′–C36′	1.491 (32)
C36–C37	1.373 (29)	C36′–C37′	1.365 (24)
C32–C37	1.435 (27)	C32′–C37′	1.441 (28)
	Bond Angles		
C32–O6–Re	133.0 (11)	C32′–O6′–Re′	135.5 (15)
C33–C32–O6	110.9 (16)	C33′–C32′–O6′	113.9 (17)
C37–C32–O6	122.3 (14)	C37′–C32′–O6′	123.6 (19)
C32–C33–N2	121.2 (18)	C32′–C33′–N2′	117.7 (16)
C34–C33–N2	128.6 (15)	C34′–C33′–N2′	129.6 (23)

cm^{-1}, *tert*-butyl stretching frequencies at 2960, 2912, and 2872 cm^{-1}, carbonyl stretching frequencies at 2011, 1921, and 1891 cm^{-1}, intense bands at 1481, 1420, 1363, 1269, 1257, and 1241 cm^{-1}, and bands of medium intensity at 1531, 1451, 1410, 1395, 1287, and 1205 cm^{-1}. All bands below 1200 cm^{-1} were of weaker intensity. Presence of the imine nitrogen stretch was used in collaboration with mass spectral and elemental analysis data to confirm identity and mode of coordination of the *o*-iminophenolate ligand.

The complex is dark maroon due to intense absorptions in the visible region of the spectrum, and this behavior is similar to that of a number of $M^{II}(Cat\text{-}N\text{-}BQ)_2$ complexes,[4] rhenium catecholate,[8] and semiquinone[12] complexes. In methylene chloride solution, $Re(CO)_3(C_{14}H_{21}NO)(C_{28}H_{39}NO_2)$ shows bands at 292 (11 000 L mol^{-1} cm^{-1}), 352 (sh), 386 (sh), 402 (14 000 L mol^{-1} cm^{-1}), 482 (9900 L mol^{-1} cm^{-1}), and 514 (sh) nm.

Simple electron-impact mass spectroscopy of the complex gave two parent ion peaks at m/e 909.4 and 911.4, corresponding to complex molecules containing the ^{185}Re and ^{187}Re isotopes. Exact mass calculation for the complex of formula $ReC_{45}H_{60}N_2O_6$ gave values of 909.398 and 911.401 for the ^{185}Re and ^{187}Re isotopes, respectively, confirming the presence of two nitrogen atoms per molecule. Elemental analysis of carbon, hydrogen, and nitrogen also confirmed these results.

Magnetism and EPR of $Re(CO)_3(C_{14}H_{21}NO)(C_{28}H_{39}NO_2)$. As a d^5-Re(II) complex coordinated to two anionic radical ligands, the complex exhibits strong antiferromagnetic coupling, giving a solid-state magnetic moment of 1.31 (2) μ_B at room temperature. This value is significantly less than the expected spin-only value for one unpaired electron and could reflect the effect of strong spin–orbit coupling. Antiferromagnetic coupling is believed to occur between the unpaired electron on rhenium with the radical localized on C32 of the *o*-iminophenolate ligand. The isotropic room-temperature EPR spectrum of this complex shown in Figure 3a confirms the presence of a ligand localized radical. The six-line signal arising from coupling to the $I = {}^5/_2$ ^{185}Re and ^{187}Re nuclei is centered about a $\langle g \rangle$ value of 2.0020 and shows rhenium hyperfine coupling of 27.6 G (pentane). Rhenium hyperfine coupling of this magnitude is consistent with ligand-localized radicals, and the nitrogen hyperfine coupling of 8.1 G confirms this charge distribution.

Similarities between the room-temperature EPR spectrum of the title compound and the spectrum of previously characterized $Re(CO)_4(C_{28}H_{39}NO_2)$ also confirm localization of the radical on the phenoxazinyl ligand.[9] Spectral parameters for the tetracarbonyl species obtained in toluene at room temperature were given as $a_{Re} = 32$ G and $a_N = 8.5$ G, and correspond very well to those obtained for the tricarbonyl *o*-iminophenolate complex.

Examination of the spectral lines in pentane over the temperature range +30 to −110 °C showed no further coupling at low temperatures. At +30 °C hyperfine coupling to hydrogen can be resolved as shown in Figure 3b. As the temperature of the solution is described, resoltuion of the nitrogen hyperfine coupling is lost at −70 °C. Hyperfine lines due to the rhenium nuclei coalesce to give four lines at −110 °C as shown in Figure 3c; however, the origin of the four-line pattern is unclear. Examination of the isotropic spectrum in toluene over the temperature range +20 to +100 °C showed irreversible dissociation of the phenoxazinyl radical ligand beginning at +60 °C. Figure 4 shows the isotropic room-temperature spectrum of this radical ligand obtained after performing a high-temperature EPR study on a pure sample of $Re(CO)_3(C_{14}H_{21}NO)(C_{28}H_{39}NO_2)$. The spectrum is centered about a $\langle g \rangle$ value of 2.0021 with nitrogen hyperfine coupling of 7.73 G and hydrogen hyperfine coupling of 2.63 and 3.88 G. These values correspond well to the spectral parameters given for the 1-hydroxy-2,4,6,8-tetra-*tert*-butylphenoxazine radical: $a_N = 7.67$ G; $a_{H3} = 3.81$ G; $a_{H7} = 4.17$ G; $a_{H9} = 2.63$ G; $\langle g \rangle = 2.0029$ (benzene).[13] Hyperfine coupling of the H7 proton could not be resolved in the experimentally obtained spectrum.

Electrochemistry on $Re(CO)_3(C_{14}H_{21}NO)(C_{28}H_{39}NO_2)$. Solutions prepared with $Re(CO)_3(C_{14}H_{21}NO)(C_{28}H_{39}NO_2)$ in

(12) deLearie, L. A.; Pierpont, C. G. *J. Am. Chem. Soc.* **1987**, *109*, 7031.
(13) Stegmann, H. B.; Scheffler, K. *Chem. Ber.* **1968**, *101*, 262.

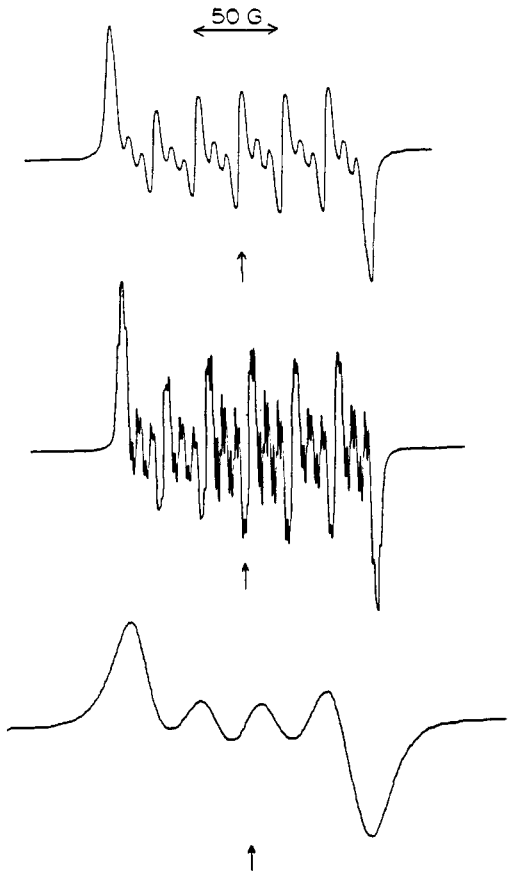

Figure 3. Isotropic EPR spectra of $Re(CO)_3(C_{14}H_{21}NO)(C_{28}H_{39}NO_2)$. Part a (top) shows the room-temperature spectrum obtained in pentane solution. The spectrum is centered about a $\langle g \rangle$ value of 2.0020 and shows Re hyperfine coupling of 27.6 G and N coupling of 8.1 G. Part b (middle) shows the spectrum obtained in toluene solution at +30 °C showing H hyperfine resolution, and part c (bottom) shows the spectrum obtained in pentane at −110 °C, showing coalescence of the six Re hyperfine lines into four lines.

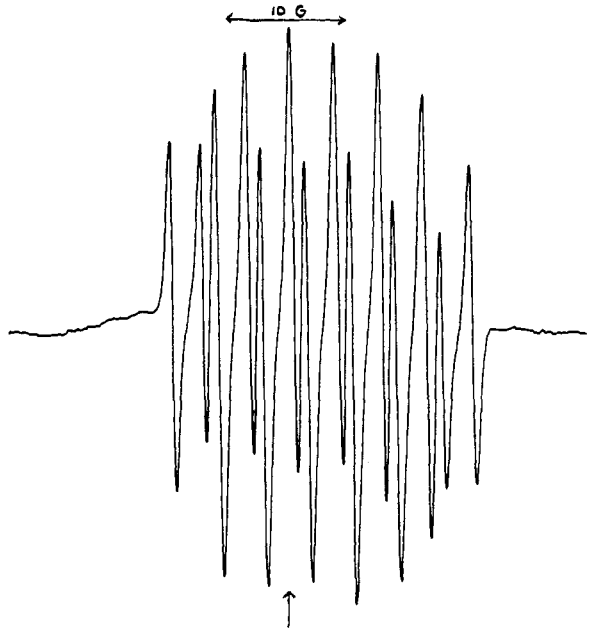

Figure 4. Isotropic EPR spectrum of the free 1-hydroxy-2,4,6,8-tetra-*tert*-butylphenoxazine radical obtained after heating a toluene solution of $Re(CO)_3(C_{14}H_{21}NO)(C_{28}H_{39}NO_2)$. The spectrum is centered about a $\langle g \rangle$ value of 2.0021 and shows N hyperfine coupling of 7.73 G and H coupling of 2.63 and 3.88 G.

methylene chloride were studied by using cyclic voltammetry and controlled-potential electrolysis. The complex undergoes two

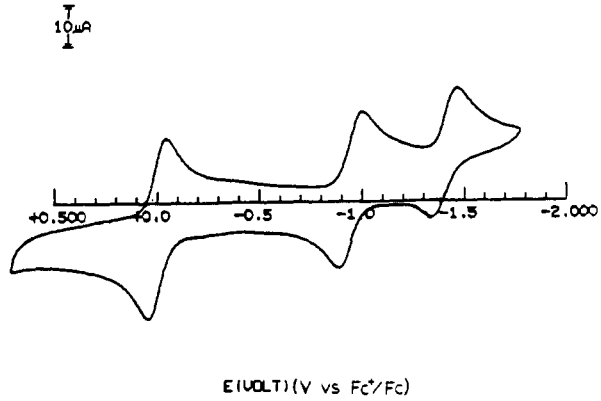

Figure 5. Cyclic voltammogram of $Re(CO)_3(C_{14}H_{21}NO)(C_{28}H_{39}NO_2)$ obtained in methylene chloride solution at a scan rate of 200 mV/s. Two reversible one-electron reductions were found to occur at −0.96 and −1.41 V vs. Fc/Fc^+. A reversible one-electron oxidation was found to occur at −0.01 V vs Fc/Fc^+.

reversible reductions and one reversible oxidation as shown in Figure 5. The first reduction occurs at −0.96 V, and the second at −1.41 V, both referenced to the Fc/Fc^+ couple. The oxidation was found to occur at −0.01 V vs Fc/Fc^+. Peak separations for all redox couples were consistent with one-electron processes at all scan rates, and results from electrolysis confirmed these values.

Oxidation of the complex most likely occurs at the metal because oxidation of either quinone derivative ligand would result in ligands having "benzoquinone-like" structures with double carbon–oxygen and carbon–nitrogen bonds. Such oxidized forms of these ligands would be poor donors, and complex dissociation would likely occur, leading to irreversible electrochemical behavior. Therefore the one-electron-oxidation product contains trivalent rhenium with a d^4 configuration. Electrolytic oxidation produced a dark green complex that has not been isolated to date.

The first reduction could occur at either of the ligands or at the metal center. Both anionic radical ligands in the neutral complex could be further reduced to their dianionic forms, which would likely be strong donors to the metal, and reversible electrochemical behavior could result. Reduction of divalent rhenium to the monovalent oxidation state could also result in reversible behavior. The second reduction could again occur at either ligand, if not previously reduced in the first reduction, or at the metal. Electrolytic reduction by one electron gave a reddish brown product, and reduction by two electrons gave a purple product, neither of which have been isolated.

Discussion

The complex $Re(CO)_3(C_{14}H_{21}NO)(C_{28}H_{39}NO_2)$ is unique. Mononuclear complexes of divalent rhenium are rare, and coordination of two different radical ligands to a single metal is also unique. The metal oxidation state has been inferred from the EPR spectra of the complex and from the structural features of the *o*-iminophenolate and phenoxazinyl ligands. Identity of the *o*-iminophenolate ligand was confirmed by both elemental analysis and mass spectroscopy, which showed the presence of two nitrogen atoms per complex molecule; one nitrogen atom in both the phenoxazinyl and iminophenolate ligands. Coordination of the *o*-iminophenolate ligand through the oxygen atom was decided due to the presence of a sharp imine N–H stretching vibration at 3204 cm^{-1} in the infrared spectrum. This vibration would have been shifted to higher energy for the O–H stretching vibration if the phenolate oxygen atom were uncoordinated.

Intramolecular coupling of unpaired metal and ligand electrons is an important aspect of transition-metal quinone chemistry. Antiferromagnetic coupling is often observed in these compounds, such as in $Cr^{III}(3,5\text{-DBSQ})_3$, in which the three metal d electrons are fully coupled to the three semiquinone radicals, resulting in a diamagnetic ground state.[14] Within quinone complexes of

(14) Buchanan, R. M.; Claflin, J.; Pierpont, C. G. *Inorg. Chem.* **1983**, *22*, 2552.

second- and third-row transition metals, localization of electrons in both discrete metal and semiquinone orbitals is seldom seen due to the larger energy separation between ligand and metal orbitals. As a result, electrons pair in the lowest energy orbitals with any remaining unpaired electrons being localized either on the metal, as in $Re^{VI}(3,5\text{-}DBCat)_3$,[8] or on the ligand, as in $Re_2(CO)_7(PhenSQ)_2$.[12] Coordination of quinones to divalent rhenium has not previously been observed, and all mononuclear complexes of the metal in this oxidation state are paramagnetic with metal-localized radicals. However, a different behavior is observed in the divalent rhenium compound $Re(CO)_3(C_{14}H_{21}NO)(C_{28}H_{39}NO_2)$. Structural features of the iminophenolate ligand clearly show radical localization within the carbonyl region of this ligand, and strong antiferromagnetic coupling to the unpaired electron on rhenium results in a paramagnetic complex with radical localization on the phenoxazinyl ligand. EPR spectral data on the compound corroborate well with this charge distribution, definitively showing radical localization on the phenoxazinyl ligand.

Monodentate coordination of the iminophenolate ligand is also unique. Previous crystallographic characterization of Fe(saloph)CatH showed similar monodentate coordination of a catecholate ligand.[9c] The saloph ligand in this iron(III) complex occupied the four basal positions of a square pyramid and prevented chelation of catechol. In the rhenium complex, three carbonyl ligands occupy facial positions and the iminophenolate ligand could chelate upon cleavage of one carbonyl ligand. However, all attempts to induce further carbonyl cleavage, either by photolysis or reaction with trimethylamine *N*-oxide, were unsuccessful, and no bidentate coordination of the iminophenolate ligand was observed.

Formation of both radical ligands in the title compound clearly involves Schiff-base condensation reactions of 3,5-di-*tert*-butylsemiquinone and ammonia. These reactions were also proposed for formation of the biquinone Cat-N-BQ ligand (see Scheme I), and Girgis suggested that due to steric constraints only the 2,4-di-*tert*-butyl-iminoquinone isomer would be formed in the initial condensation reaction.[4b] However, complexation of 3,5-di-*tert*-butyliminophenolate to rhenium in $Re(CO)_3(C_{14}H_{21}NO)(C_{28}H_{39}NO_2)$ is evidence that both iminoquinone isomers are formed in these initial reactions. Steric constraints would have an effect on further reactions of the iminoquinones involved in formation of Cat-N-BQ ligands with only the 2,4-substituted isomer having the correct conformation to react through further Schiff-base condensation with 3,5-di-*tert*-butylcatechol. 3,5-Di-*tert*-butyliminoquinone is likely a side product in reactions giving $M^{II}(Cat\text{-}N\text{-}BQ)_2$ complexes, but in reactions with $Re(CO)_5Br$, this ligand reacts further with rhenium to give the isolated product.

Formation of 1-hydroxy-2,4,6,8-tetra-*tert*-butylphenoxazinylate radicals are known to occur through additional reactions of Cat-N-BQ anions in basic media.[13] These reactions were not previously outlined but likely involve initial addition of the oxygen on one quinone ring to the carbon positioned ortho to the imine functionality on the other ring, followed by deprotonation and oxidation in air. Coordination of this radical to a variety of organometallic fragments, including $Re(CO)_4$, has previously been studied by EPR spectroscopy, and chelation to metals through the deprotonated hydroxy oxygen atom and the nitrogen atom was proposed.[10] Crystallographic characterization of $Re(CO)_3(C_{14}H_{21}NO)(C_{28}H_{39}NO_2)$ is the first structural characterization of this ligand and confirms bidentate coordination to metals.

Acknowledgment. This research was supported by the National Science Foundation under Grants CHE 85-03222, CHE 88-09923, and CHE 84-12182 (X-ray instrumentation).

Supplementary Material Available: Tables containing details of the structure determination and refinement, anisotropic thermal parameters, and a complete list of bond distances and angles for $Re(CO)_3(C_{14}H_{21}NO)(C_{28}H_{39}NO_2)$ (12 pages); a listing of observed and calculated structure factors (23 pages). Ordering information is given on any masthead page.

Contribution from the Department of Chemistry, Northwestern University, Evanston, Illinois 60208

Mixed-Metal Selenides: Synthesis and Characterization of the $Ni(Se_2)(WSe_4)^{2-}$ and $M(WSe_4)_2^{2-}$ (M = Ni, Pd) Anions

Mohammad A. Ansari, Chung-Nin Chau, Charles H. Mahler, and James A. Ibers*

Received June 24, 1988

Reaction of $[NH_4]_2[WSe_4]$ dissolved in DMF with a suspension of $Ni(acac)_2$ in DMF in the presence of $[PPh_4]Cl$ affords $[PPh_4]_2[Ni(Se_2)(WSe_4)]$. A similar reaction involving $NiCl_2(PPh_3)_2$ in place of $Ni(acac)_2$ affords $[PPh_4]_2[Ni(WSe_4)_2]$, while the use of $PdCl_2(C_6H_5CN)_2$ affords $[PPh_4]_2[Pd(WSe_4)_2]$. The $Ni(Se_2)(WSe_4)^{2-}$ ion shows ^{77}Se NMR resonances at δ 1399, 855, and 608 ppm expected for the structure found in the solid state consisting of a square-planar Ni center bound to a side-on Se_2 group and to a nearly tetrahedral WSe_4 group ($[PPh_4]_2[Ni(Se_2)(WSe_4)]$, $Z = 4$, $P2_1/n$, $a = 14.222$ (6) Å, $b = 17.168$ (7) Å, $c = 19.976$ (8) Å, $\beta = 110.3$ (2)°, $R(F^2) = 0.076$ for 9932 observations). This ion has no known sulfide analogue. The $M(WSe_4)_2^{2-}$ ions (M = Ni, Pd) are closely analogous to the known $Ni(WS_4)_2^{2-}$ ion and show two ^{77}Se NMR resonances (Ni 1628, 994 ppm; Pd 1673, 1135 ppm) consistent with the structure found in the solid state for $[PPh_4]_2[Ni(WSe_4)_2]$ in which the square-planar Ni center is bound to two nearly tetrahedral WSe_4 centers ($Z = 1$, $P\bar{1}$, $a = 9.347$ (3) Å, $b = 12.410$ (3) Å, $c = 12.557$ (3) Å, $\alpha = 65.76$ (1)°, $\beta = 84.61$ (2)°, $\gamma = 69.83$ (2)°, $R(F^2) = 0.090$ for 7295 observations). While the $Pd(WSe_4)_2^{2-}$ ion is stable in DMF solution at room temperature, the corresponding $Ni(WSe_4)_2^{2-}$ ion decomposes to form the $Ni(Se_2)(WSe_4)^{2-}$ ion.

Introduction

Soluble metal sulfides[1-3] and mixed-metal sulfides[4-6] continue to be of interest. Among mixed-metal sulfides, M-Fe-S systems (M = Mo, W) have attracted the most attention because of their relevance to the nitrogenase problem.[7,8] The ligating behavior of MS_4^{2-} toward M′ to form $M'(MS_4)_2^{2-}$ (M = Mo, W; M′ = Fe, Co, Ni, Pd, Pt, Zn, Cd, Hg) has been studied in detail.[1,9] Some other heteropolythiometalates, e.g., $FeX_2(MS_4)^{2-}$ (X = Cl, PhS), have also been reported.[10,11] The corresponding selenium

(1) Müller, A.; Diemann, E.; Jostes, R.; Bögge, H. *Angew. Chem., Int. Ed. Engl.* **1981**, *20*, 934-955.
(2) Müller, A. *Polyhedron* **1986**, *5*, 323-340.
(3) Draganjac, M.; Rauchfuss, T. B. *Angew. Chem., Int. Ed. Engl.* **1985**, *24*, 742-757.
(4) Averill, B. A. *Struct. Bonding (Berlin)* **1983**, *53*, 59-103.
(5) Coucouvanis, D.; Baenziger, N. C.; Simhon, E. D.; Stremple, P.; Swenson, D.; Kostikas, A.; Simopoulos, A.; Petrouleas, V.; Papaefthymiou, V. *J. Am. Chem. Soc.* **1980**, *102*, 1730-1732.
(6) McDonald, J. W.; Friesen, G. D.; Newton, W. E. *Inorg. Chim. Acta* **1980**, *46*, L79-80.
(7) Hughes, M. N., Ed. *The Inorganic Chemistry of Biological Process*; Wiley: New York, 1984.
(8) Spiro, T. G., Ed. *Molybdenum Enzymes*; Wiley-Interscience: New York, 1986.
(9) Callahan, K. P.; Piliero, P. A. *Inorg. Chem.* **1980**, *19*, 2619-2626.
(10) Coucouvanis, D.; Simhon, E. D.; Swenson, D.; Baenziger, N. C. *J. Chem. Soc., Chem. Commun.* **1979**, 361-362.

0020-1669/89/1328-0650$01.50/0 © 1989 American Chemical Society